Check for updates

NEUROINFLAMMATION

Deletion of the X-chromosomal gene *Kdm6a* in microglia of female mice ameliorates neuroinflammation and restores translatome profiles

Yuichiro Itoh, Noriko Itoh, Sophia Wendin, Nadya Higgins, Rhonda R. Voskuhl*

Copyright © 2025 The Authors, some rights reserved; exclusive licensee American Association for the Advancement of Science. No claim to original U.S. Government Works

Women are more susceptible to multiple sclerosis (MS) than men, with a reported incidence ratio of ~3:1. *Kdm6a* is an X-chromosomal gene that escapes X inactivation, leading to higher expression of the histone demethylase KDM6A in females compared with males. Here, we focused on the role of *Kdm6a* in microglia in MS because this cell type plays a key role in the neuropathology of MS. *Kdm6a* was selectively deleted from microglia in experimental autoimmune encephalomyelitis (EAE) mice, an established model of MS. Deletion of *Kdm6a* in microglia ameliorated pathology, reduced the expression of disease-associated markers, increased the expression of resting microglial markers, and reversed other translatome changes in spinal cord tissues of female EAE mice. Deletion of *Kdm6a* in microglia had only very minor effects on EAE in male mice. The diabetes medicine metformin, which also blocks KDM6A's histone demethylase activity, ameliorated EAE in females, but not males, and normalized translatome profiles in microglia. CUT&RUN and sequencing analysis of microglial nuclei identified genes bound by KDM6A. When combined with translatomic analysis, this revealed correspondence between KDM6A protein binding and gene expression changes. Transcriptomic analysis of human microglia confirmed the higher expression of *KDM6A* in women compared with men and revealed that more microglial genes were dysregulated in women than in men with MS. Our results suggest that *KDM6A* might contribute to sex differences in susceptibility to MS.

INTRODUCTION

Multiple sclerosis (MS) is an autoimmune and neurodegenerative disease. Lymphocytes and macrophages in peripheral blood infiltrate the central nervous system (CNS), resulting in the activation of microglia and astrocytes, demyelination, and axonal damage in white matter lesions, with glial activation and synaptic loss in gray matter. Its etiology is not completely understood, although genetic and environmental factors have been proposed (*1*–*3*). The ratio of females to males with MS is ~3:1 with more relapsing disease in females, whereas males demonstrate a more progressive disease course (*4*). Microglia, the resident immune cells of the CNS, are thought to play a key role in neurodegeneration in MS (*5*, *6*), and sex differences in microglia during health, aging, and neurodegenerative diseases are an area of active investigation (*7*–*13*).

Sex differences in microglia can be caused by differential effects of sex hormones (estrogen versus testosterone), sex chromosomes (XX versus XY), or both (*4*, *14*–*19*). The Genotype Tissue Expression Project (GTEx) found that 37% of all genes exhibit sex-biased expression, which is tissue specific (*20*–*22*), but how this occurs is unclear. It could be due to estrogens acting on estrogen response elements of autosomal genes (*23*–*25*) or due to epigenetic effects of sex chromosome genes (*26*, *27*). Factors influencing sex differences can also change across the life span. For example, sex hormone concentrations in blood are high from puberty to midlife but decrease with menopause and andropause (*19*). In addition, DNA methylation is affected by aging (*28*). Thus, the balance between the effect of sex hormones versus sex chromosomes (*29*, *30*) on gene expression is likely to be dynamic across the life span (*19*).

Regarding sex chromosome genes, females (XX) have two X chromosomes, whereas males (XY) have only one. This twofold genomic dose difference in X-chromosomal genes in females is compensated by random inactivation of one X chromosome, leading to similar expression of X genes in both sexes (*31*). There are several X genes that escape X inactivation. One of these X-escapee genes, *Kdm6a* (*lysine demethylase 6A*; also known as *Utx*), has higher expression in females compared with males (*32*, *33*). Histone demethylase KDM6A protein specifically mediates the removal of repressive trimethylation on histone H3 lysine 27 (H3K27me3) to expose a region of chromatin. KDM6A associates with the methyltransferase KMT2D (lysine methyltransferase 2D) in the same protein complex (*34*), and KMT2D adds the activating H3K4me3 histone mark (*35*). This complex modulates gene expression by histone modifications that make the chromatin transcriptionally permissive in a cell lineage–specific manner (*36*, *37*). Thus, a dose effect of the X-chromosomal gene *Kdm6a*, namely, two copies in females and one in males, can influence genome-wide expression.

Here, we selectively deleted *Kdm6a* in microglia to determine sex-specific effects in experimental autoimmune encephalomyelitis (EAE) mice (*38*, *39*). Toward translation, metformin treatment was used to examine the therapeutic effects of KDM6A inhibition on EAE mice. Last, *KDM6A* expression in microglia from women and men with MS and healthy controls was compared.

RESULTS

Microglial specificity of *Tmem119*-Cre/ERT2 transgene

Before examining the effect of selective deletion of *Kdm6a* in microglia during EAE, we first chose an optimal tamoxifen-inducible microglial Cre mouse line. *Cx3cr1*-Cre/ERT2 (*40*) and *Tmem119*-Cre/ERT2 (*41*, *42*) lines were examined for the endogenous expression of the *Cx3cr1* and *Tmem119* genes by reverse transcription

Department of Neurology, David Geffen School of Medicine, University of California, Los Angeles, Los Angeles, CA 90095, USA.
*Corresponding author. Email: rvoskuhl@mednet.ucla.edu

Downloaded from https://www.science.org at Texas A&M University, Kingsville on November 14, 2025

polymerase chain reaction (fig. S1A). The homozygous *Cx3cr1*-Cre/ERT2 line did not express *Cx3cr1* because insertion of the Cre/ERT2 fusion sequence disrupts endogenous expression of *Cx3cr1* (*40*). The *Cx3cr1*-Cre/ERT2 line had previously been used in EAE to determine the function of an unrelated gene (*43*); however, *Cx3cr1* expression is known to confer protective effects in EAE (*44*–*47*). Thus, knockout of endogenous *Cx3cr1* is a confound when determining the effect of gene deletion of *Kdm6a* in microglia during EAE. In contrast, the *Tmem119*-Cre/ERT2 line retained expression of endogenous *Tmem119* (fig. S1A). Therefore, the *Tmem119*-Cre/ERT2 line was chosen as the inducible microglial Cre line for this study.

The specificity of microglial Cre activity using the *Tmem119*-Cre/ERT2 line was examined using *Tmem119*-Cre/ERT2-RiboTag mice. In RiboTag mice, the hemagglutinin (HA)–tagged ribosomal protein is expressed under the control of Cre recombinase activity (*48*). *Tmem119*-Cre/ERT2-RiboTag mice were injected with tamoxifen for 5 consecutive days. Eight weeks later, immunohistochemistry entailed costaining with anti-HA antibody and CNS cell type–specific antibodies. Cells labeled with anti-HA were colabeled with the microglial marker P2RY12 (fig. S1B), whereas antibodies for other CNS cell types [glial fibrillary acidic protein (GFAP), astrocyte; RNA binding Fox-1 homolog 3 (RBFOX3, also known as NeuN), neuron; glutathione S-transferase pi (GSTpi), oligodendrocyte] showed no colabeling with HA (fig. S1C). To determine microglial specificity of the *Tmem119*-Cre/ERT2 line at RNA level, immunoprecipitated RNAs from *Tmem119*-Cre/ERT2-RiboTag mice were examined for expression of CNS cell type–specific genes. Microglial markers (*Cd83*, *Ptprc*, and *Tmem119*) were enriched in immunoprecipitated RNAs. In contrast, astrocyte (*Gfap*, *Aqp4*, *Aldh1l1*, and *Aldoc*), neuron (*Syp* and *Syn1*), and oligodendrocyte (*Mbp* and *Mog*) markers showed deenrichment (fig. S1D). Thus, at both the protein and RNA levels, the *Tmem119*-Cre/ERT2 line was found to drive Cre recombination specifically in microglia, supporting rigorous microglial specificity of this Cre line (*49*).

Validation of *Kdm6a* deletion in microglia

Before selectively deleting *Kdm6a* from microglia, *Kdm6a* was first shown to be highly expressed in mouse microglia, with higher abundances in females than males (fig. S2, A to D). To determine the function of *Kdm6a* in microglia, floxed *Kdm6a* mice (*Kdm6a*$^{f/f}$) were crossed with the RiboTag and *Tmem119*-Cre/ERT2 lines, making mice with three genetic modifications: floxed *Kdm6a*, RiboTag, and *Tmem119*-Cre/ERT2. In these mice, the activation of the RiboTag HA allele and the deletion of *Kdm6a* were both driven by *Tmem119*-Cre/ERT2. Thus, microglial expression of KDM6A protein could be identified by colabeling with anti-HA antibody and anti-KDM6A antibody. Immunofluorescence staining of KDM6A protein from *Tmem119*-Cre/ERT2-RiboTag [wild-type (WT)] and *Tmem119*-Cre/ERT2-*Kdm6a*$^{f/f}$-RiboTag [conditional knockout (cKO)] mice are shown in fig. S3A. WT mice showed KDM6A protein expression (red) in the HA-labeled microglia (green), whereas this was absent in the cKO mice (fig. S3A). On the other hand, KDM6A expression in the nuclei of nonmicroglial cells showed no decrease in the microglial *Kdm6a* cKO (fig. S3, A and B). This was further evaluated by the functional activity of KDM6A protein, namely H3K27me3 histone demethylase activity. Compared with WT animals, the amounts of H3K27me3 in the nuclei of microglia were higher in cKO mice (red) (fig. S3, C and D).

Deletion of *Kdm6a* in microglia is protective in female EAE mice

To examine the function of the *Kdm6a* deletion in microglia during disease, active EAE (*38*) was induced in female *Tmem119*-Cre/ERT2-*Kdm6a*$^{f/f}$ (cKO) and littermate *Tmem119*-Cre/ERT2 negative control mice (WT). In these mice, the microglial *Kdm6a* gene was deleted with tamoxifen treatment at 2 months of age, and EAE was induced 8 weeks later. EAE clinical scores of cKO mice were lower than those in WT mice, demonstrating that the deletion of *Kdm6a* in microglia was protective (Fig. 1A). This protective effect of *Kdm6a* deletion in microglia was further confirmed with additional EAE experiments in females (table S1). When peripheral immune cells were isolated from lymph nodes of mice in an early stage of EAE (day 15) and stimulated in vitro with myelin oligodendrocyte glycoprotein (MOG), there were no differences in cytokine abundances when comparing cKO versus WT mice—interleukin-2 (IL-2) ($P = 0.779$), tumor necrosis factor ($P = 0.397$), interferon ($P = 0.152$), IL-17 ($P = 0.397$), and IL-4 ($P = 0.320$)—demonstrating that peripheral immune responses to MOG were not affected by *Kdm6a* cKO in microglia. Together, these targeted loss-of-function study results revealed that the presence of *Kdm6a* in microglia is deleterious during EAE.

Neuropathology of the spinal cords in mice with EAE also revealed that selective deletion of *Kdm6a* induced neuroprotective effects. Specifically, a marker of axonal damage, amyloid-β precursor protein (APP), was decreased (Fig. 1B, $P = 0.036$), whereas a marker of intact axons, neurofilament 200kD (NF200), was increased (Fig. 1C, $P = 0.002$) during EAE in the cKO compared with WT mice. In addition, T cells in spinal cord white matter were reduced in EAE cKO mice (Fig. 1D, $P = 0.0006$), and there was more myelin observed in EAE cKO mice compared with WT mice (Fig. 1E, $P = 0.021$). Together, these results showed that selective deletion of *Kdm6a* in microglia ameliorated EAE at both the clinical and neuropathologic levels.

Deletion of *Kdm6a* in microglia alters the microglial translatome

RNA sequencing (RNA-seq) data of fluorescence-activated cell-sorted spinal cord microglia from EAE and healthy controls were obtained from Gene Expression Omnibus (GEO; GSE154228) (*50*). Resting microglial markers were down-regulated in EAE, whereas disease-associated microglial marker genes were up-regulated (Fig. 2A) (*51*, *52*). To examine the effect of microglial *Kdm6a* deletion on gene expression in microglia in vivo, EAE was induced in *Tmem119*-Cre/ERT2-RiboTag (WT) and *Tmem119*-Cre/ERT2-*Kdm6a*$^{f/f}$-RiboTag (cKO) female mice, and microglial RNAs were isolated from spinal cords using HA pull-down, followed by RNA-seq. Differential gene expression analysis was performed comparing microglial translatomes in the WT versus the microglial *Kdm6a* cKO mice using edgeR, and 1465 genes were differentially translated between WT and cKO mice [table S2; threshold: false discovery rate (FDR) < 0.1, log counts per million > 1, and log fold change higher than 0.5 or lower than −0.5]. In microglia of *Kdm6a* cKO mice with EAE, three resting microglial markers (*P2ry12*, *Siglech*, and *Sall1*) were up-regulated, whereas disease-associated microglial markers [*Gpnmb* (*glycoprotein Nmb*) and *Siglec1*] (*51*) were down-regulated (Fig. 2B). In healthy mice, disease-associated microglial markers showed no difference between cKO and WT, whereas four resting microglial markers showed a slight increase in cKO mice (Fig. 2C, FDR < 0.1). Comparison of translatomes in Fig. 2 (A and B) showed that 68 down-regulated

Downloaded from https://www.science.org at Texas A&M University, Kingsville on November 14, 2025

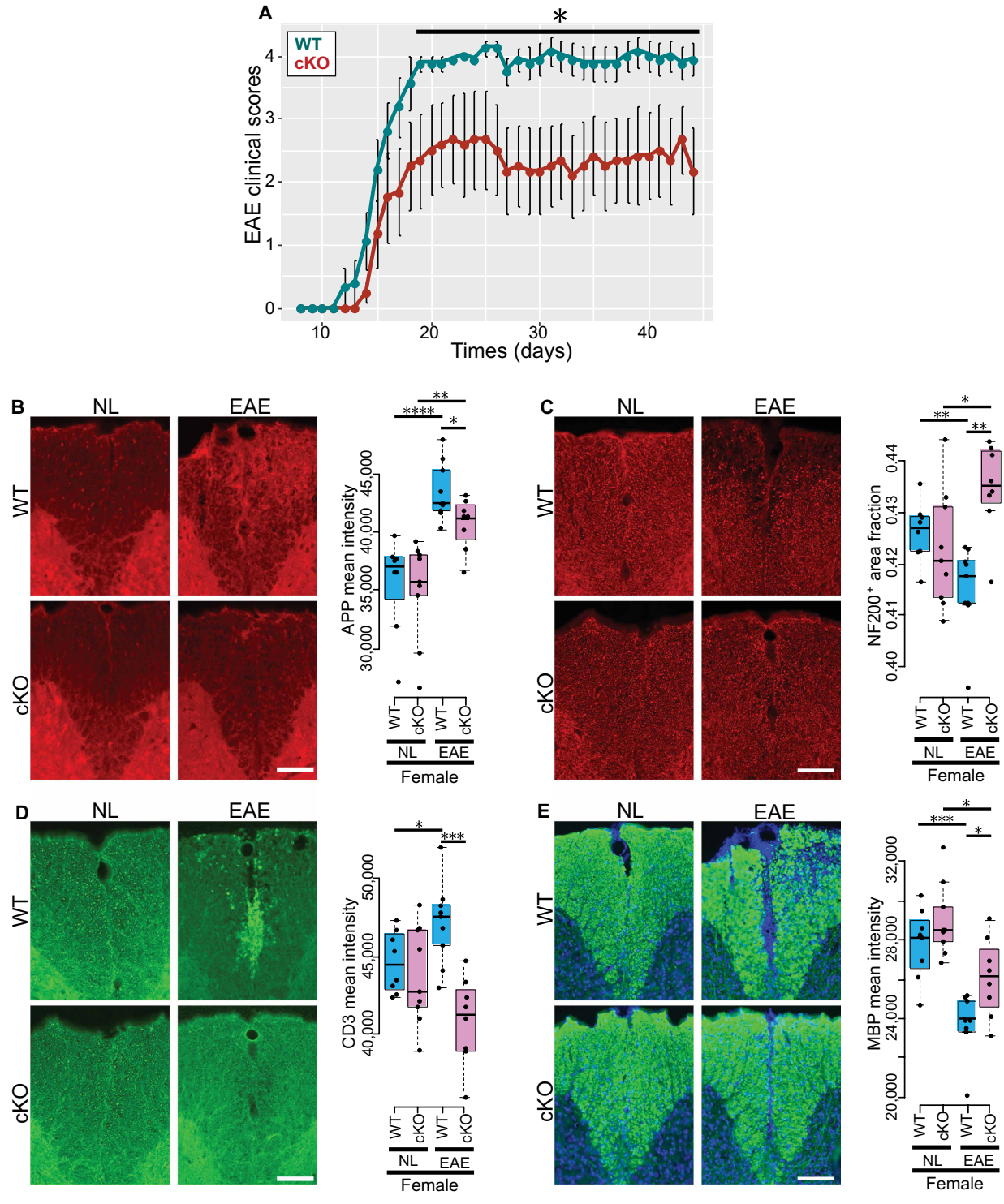

Fig. 1. *Kdm6a* deletion from microglia has protective effects in female EAE mice. (**A**) *Tmem119*-Cre/ERT2$^{+/-}$-*Kdm6a*$^{f/f}$ (cKO) and *Tmem119*-Cre/ERT2$^{-/-}$-*Kdm6a*$^{f/f}$ (WT) female mice were treated with tamoxifen to induce microglia-specific knockout of *Kdm6a*, and 8 weeks later, chronic EAE was induced. The graph shows EAE severity scores for *Tmem119*-Cre/ERT2$^{+/-}$-*Kdm6a*$^{f/f}$ (cKO) and *Tmem119*-Cre/ERT2$^{-/-}$-*Kdm6a*$^{f/f}$ (WT) female mice. $n = 8$ WT and $n = 6$ cKO. Repeated-measures one-way ANOVA, $^{*}P < 0.05$. (**B** to **E**) Representative immunofluorescence images of ventral spinal cord tissues from WT and cKO mice that underwent EAE or healthy normal control (NL) (left) and box-and-whisker plots showing quantifications of protein expression (right) for APP (B) (red), NF200 (C) (red), CD3 (D) (green), and MBP (E) [green; nuclei stained with 4′,6-diamidino-2-phenylindole (DAPI) in blue]. Double staining was performed: NF200/CD3 and APP/MBP. Scale bars, 100 μm. $n = 8$ (WT NL), $n = 9$ (cKO NL), $n = 9$ (WT EAE), and $n = 8$ (cKO EAE). For the box-and-whisker plots, the boxes indicate the medians and 25th to 75th percentile ranges, and the whiskers extend to a maximum of 1.5 times the interquartile ranges beyond the boxes. Mann-Whitney *U* test, $^{*}P < 0.05$; $^{**}P < 0.01$; $^{***}P < 0.001$; $^{****}P < 0.0001$.

Downloaded from https://www.science.org at Texas A&M University, Kingsville on November 14, 2025

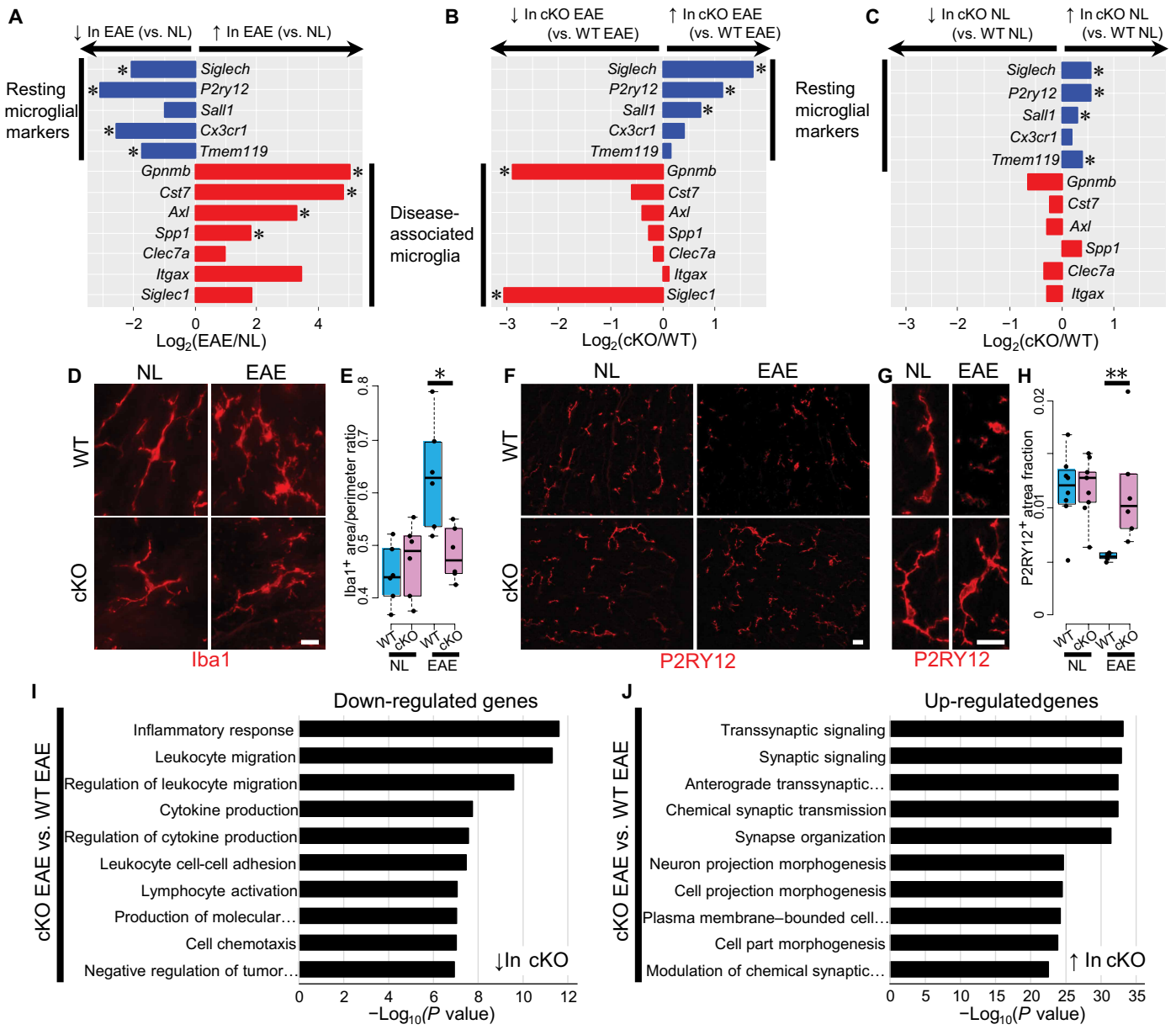

Fig. 2. The effect of microglial *Kdm6a* deletion on the translatome of microglia in female EAE mice. (**A** to **C**) Gene expression changes in markers of resting microglia (blue) and markers of DAM (red). (A) EAE ($n = 6$) versus healthy mice (NL; $n = 4$), (B) microglial *Kdm6a* cKO versus WT mice (both with EAE), (C) microglial *Kdm6a* cKO versus WT mice (both in NL). Asterisks indicate FDR < 0.1 (edgeR). (**D**) Representative immunofluorescence images of spinal cord white matter (normal appearing, without lesions) from WT and cKO mice that underwent EAE or healthy normal control (NL) showing Iba1$^+$ microglia. (**E**) Area/perimeter ratios of Iba1$^+$ microglia for groups as in (D). $n = 6$ in each. (**F**) Representative immunofluorescence images for tissue as in (D) showing P2RY12$^+$ microglia. (**G**) Higher magnification of images as in (F). (**H**) P2RY12$^+$ area fraction for groups as in (F). $n = 8$ each (NL) and $n = 6$ each (EAE). Scale bars, 10 μm (all images). Mann-Whitney *U* test, $^{**}P < 0.01$. (**I** and **J**) GO enrichment analysis of down-regulated (I) [FDR < 0.1 and log fold change (logFC) < −0.5] and up-regulated genes (J) (FDR < 0.1 and logFC > 0.5) in cKO EAE compared with WT EAE mice.

genes in EAE were up-regulated by the deletion of *Kdm6a* in microglia, whereas 73 up-regulated genes in EAE were down-regulated by *Kdm6a* deletion in microglia, indicating that cKO of *Kdm6a* in microglia reversed certain gene expression changes induced by EAE (fig. S4). Together, these findings indicate that the translatomes of microglia from EAE mice with selective deletion of *Kdm6a* in microglia revealed a shift away from disease-associated microglia (DAM) toward resting microglia.

Microglia were then examined at the protein level using immunohistochemistry of spinal cord sections from the microglial *Kdm6a* cKO and WT. Immunohistochemical staining for Iba1 was done, and area/perimeter ratios were determined. Because activated microglia have a large area and small perimeter, higher area/perimeter ratios indicate microglial activation (*53*). Consistent with activation of microglia during EAE, area/perimeter ratios were increased in WT EAE versus WT normal mice (Fig. 2, D and E). In contrast, area/perimeter ratios were decreased in cKO EAE compared with WT EAE mice (Fig. 2, D and E).

In addition, expression of the resting microglial marker P2RY12 was examined. P2RY12 was decreased in WT EAE compared with

Downloaded from https://www.science.org at Texas A&M University, Kingsville on November 14, 2025

WT normal mice (Fig. 2, F to H). In contrast, P2RY12 was increased in cKO EAE compared with WT EAE mice (Fig. 2, F to H). Thus, higher expression of P2RY12 at the protein level matched higher expression of *P2ry12* at the RNA level during EAE in the microglial *Kdm6a* cKO (Fig. 2B).

Next, GO (Gene Ontology) enrichment analyses of differentially translated genes showed that genes down-regulated in the cKO compared with WT mice during EAE were enriched in the inflammatory response, cytokine production, lymphocyte activation, and leukocyte migration GO categories (Fig. 2I). These inflammation pathways were not enriched in cKO healthy controls versus WT healthy controls (fig. S5, A and B). On the other hand, the genes up-regulated in the cKO mice during EAE were enriched in the synapse-related GO categories (Fig. 2J).

Last, because the *Siglec1* gene is a member of the most enriched down-regulated category, namely, the inflammatory response, immunohistochemistry analysis of the *Siglec1* gene was performed as validation. *Siglec1* is one of the DAM signature genes (*54*). SIGLEC1 has been shown to be expressed in activated microglia in EAE and MS (*52*). At the RNA level, *Siglec1* gene expression was lower in cKO compared with WT mice during EAE (Fig. 3A). At the protein level, Siglec1 protein expression in Iba1$^+$ microglia was increased in WT EAE versus WT normal, whereas Siglec1 was decreased in cKO EAE compared with WT EAE mice (Fig. 3, B and C). Together, this demonstrated that deletion of *Kdm6a* in microglia shifted microglial genes from a disease-associated phenotype to a resting phenotype during EAE.

Sex-specific effects of *Kdm6a* deletion in EAE mice

Because *Kdm6a* is an X-chromosomal gene that escapes X inactivation in females and has a gene dosage effect compared with males, additional microglial *Kdm6a* cKO versus WT experiments were done, including both female and male mice examined in parallel within the same EAE experiment. The protective effect of selective deletion of *Kdm6a* in microglia was further confirmed in two additional EAE experiments in females (cumulatively six total experiments in females), but males did not show a difference in EAE disease scores when comparing cKO to WT mice (Fig. 4, A and B, and table S3). In addition, there was no decrease in microglial activation in *Kdm6a* cKO male mice during EAE, as measured by area/perimeter ratios (fig. S6A). Neuropathology of spinal cords in male EAE mice showed a decrease in APP and increase in myelin basic protein (MBP) but no difference in NF200 and CD3 between cKO and WT mice (fig. S6, B to E).

To investigate a possible sex difference in the effect of *Kdm6a* deletion in microglia during EAE at the translatome level, an additional RNA-seq experiment was performed for female and male mice in parallel, whereby EAE was induced in both sexes at the same time. Principal components analysis (PCA) of microglial translatomes from female (WT and cKO) and male (WT and cKO) mice

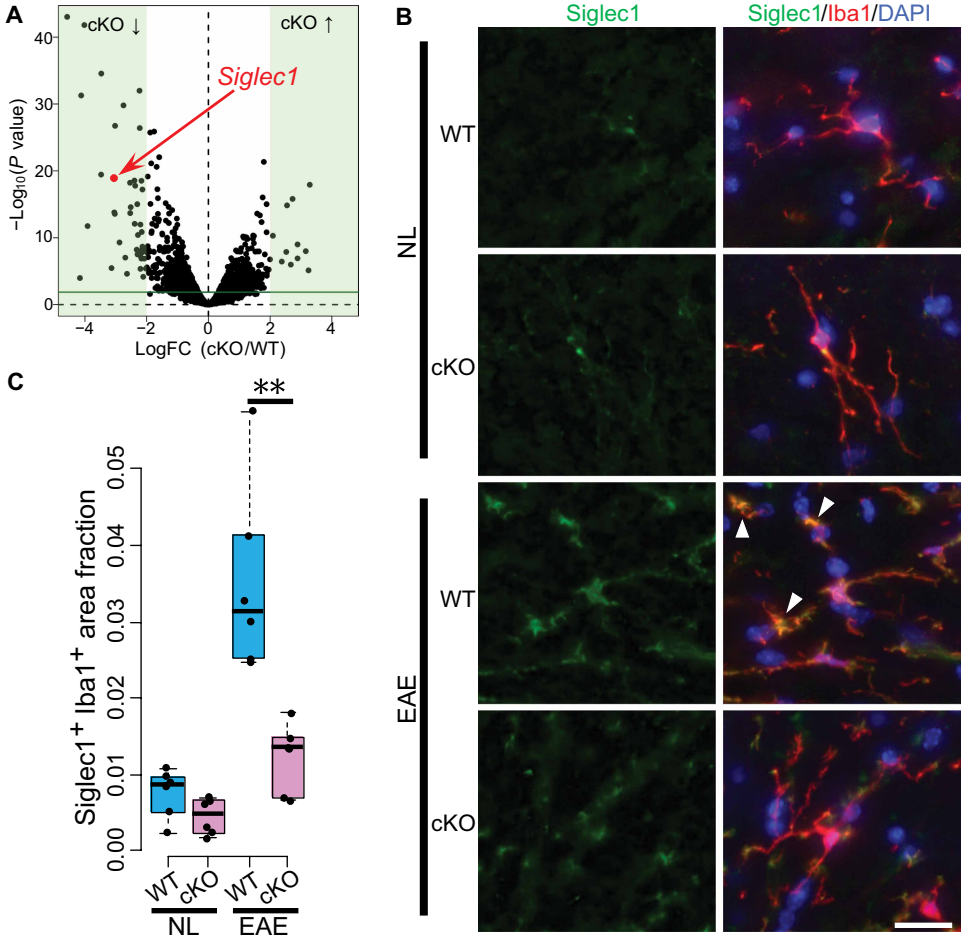

Fig. 3. Siglec1 protein was down-regulated in cKO mice during EAE. (**A**) Volcano plot depicting differentially expressed genes in cKO EAE mice compared with WT EAE mice. Green line indicates FDR = 0.1, and green shading indicates >4 fold change. The red dot highlights *Siglec1* expression. (**B**) Representative immunofluorescence images of spinal cord white matter from WT and cKO mice with or without EAE. Siglec1 protein (green) costained with Iba1 (red) and DAPI (blue). White arrowheads indicate colocalization of Siglec1 and Iba1 (yellow). Spinal cord white matter. Scale bar, 20 μm. (**C**) Quantification of microglial Siglec1 protein expression in treatment groups as in (B). $n = 6$ in each group. Mann-Whitney *U* test, $^{**}P < 0.01$.

Downloaded from https://www.science.org at Texas A&M University, Kingsville on November 14, 2025

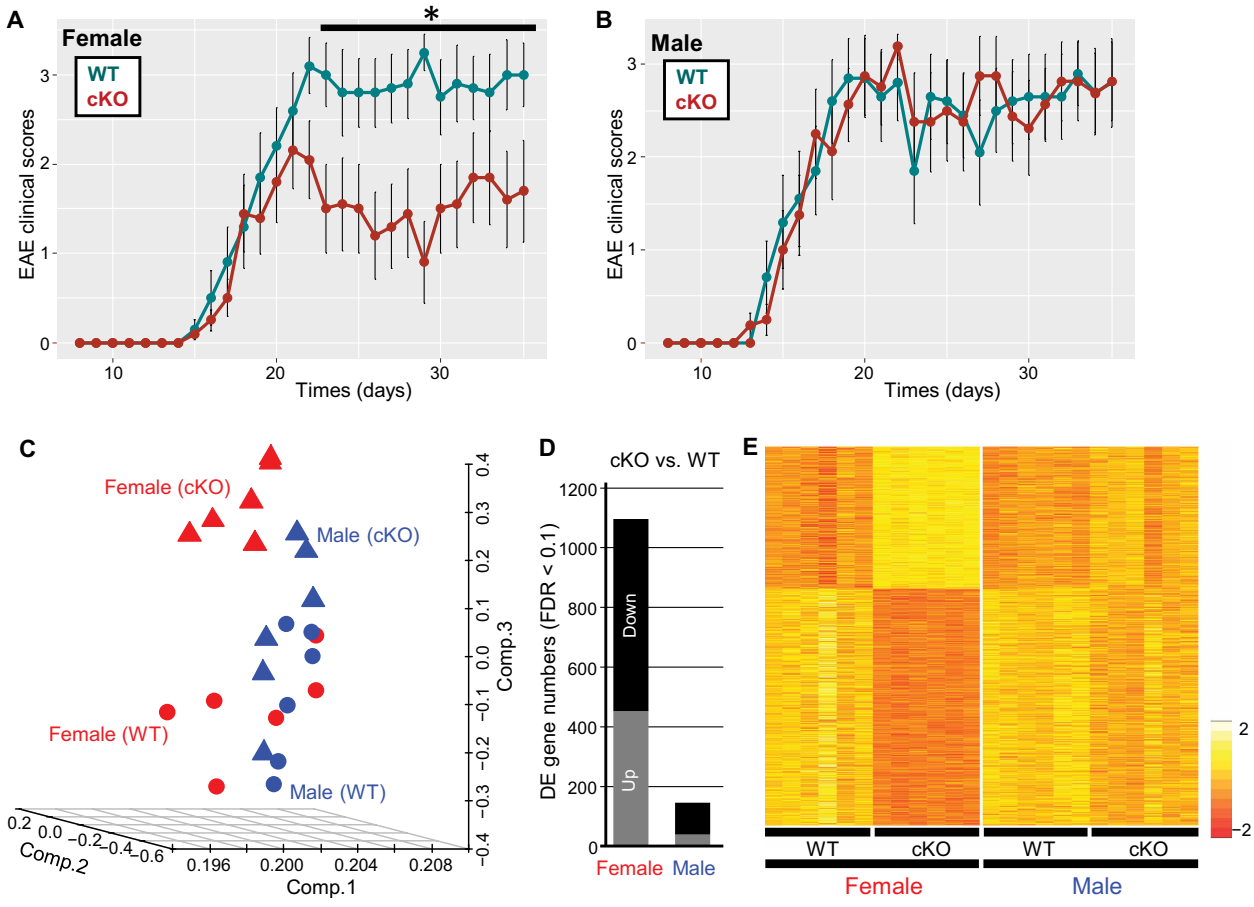

Fig. 4. *Kdm6a* deletion in microglia did not affect clinical scores in male mice with EAE. (**A** and **B**) *Tmem119*-Cre/ERT2$^{+/-}$-*Kdm6a* (cKO) and *Tmem119*-Cre/ERT2$^{-/-}$-*Kdm6a* (WT) female and male mice were treated with tamoxifen to induce microglia-specific knockout of *Kdm6a*, and 8 weeks later, chronic EAE was induced. Shown are EAE clinical scores for cKO and WT female ($n = 10$ per group) (A) and male ($n = 8$ to 10 per group) (B) mice. Repeated-measures one-way ANOVA, $^*P < 0.05$. (**C**) PCA of microglial translatome from female and male cKO and WT EAE mice. (**D**) Comparisons of differentially expressed (DE) gene numbers (cKO versus WT; FDR < 0.1 and logFC < −0.5 or logFC > 0.5) in female and male mice during EAE. Up- and down-regulated genes are shown in gray and black, respectively. (**E**) Heatmap of differentially translated genes (FDR < 0.1 and logFC < −0.5 or logFC > 0.5) for male and female samples. In males, a trend of differences in the same directions of females was observed between cKO and WT mice. Unit = *z*-score.

showed distinct separation between female cKO and female WT translatomes, whereas male cKO and male WT translatomes were not as distinctly separated (Fig. 4C). Consistent with the PCA result, differentially translated gene numbers in the comparison of cKO and WT microglia were much larger in females compared with males (Fig. 4D). This was also reflected in the heatmap of differentially translated genes in each sex (Fig. 4E).

Therapeutic effects of metformin on EAE clinical scores and the microglial translatomes in female mice

We next examined the effect of metformin treatment on pathology and the microglial translatome during EAE. Metformin is a US Food and Drug Administration (FDA)–approved drug for the treatment of diabetes with suggested antiaging properties. Metformin has multiple functions and has been shown to inhibit the histone demethylase activity of KDM6A (*55*). EAE was induced in female mice, and metformin or vehicle was used as a treatment. EAE clinical scores were reduced in metformin-treated mice (Fig. 5A and table S4), consistent with previous clinical findings by others (*56*–*58*). Immunohistochemistry on spinal cord tissues showed that Iba1 area/perimeter ratios were increased in EAE mice versus healthy controls, and this was decreased in metformin-treated versus vehicle-treated EAE mice (Fig. 5B). In addition, expression of the resting microglial marker P2RY12 was examined. P2RY12 was decreased in EAE mice compared with healthy controls, whereas P2RY12 was increased with metformin treatment of EAE mice (Fig. 5C).

RNA analysis using microglial RiboTag mice that were vehicle-treated revealed again that disease-associated microglial marker genes were up-regulated in EAE, whereas resting microglial markers were down-regulated, each compared with healthy controls (Fig. 5D). In metformin-treated EAE female mice, the disease-associated microglial marker *Gpnmb* was down-regulated, and resting microglial markers were up-regulated compared with vehicle-treated EAE mice (Fig. 5E).

Next, the effects of metformin treatment on microglia during EAE were examined at the genome-wide level by treating microglial RiboTag mice with metformin. The top 500 differentially translated genes between EAE and healthy controls were labeled red when

Downloaded from https://www.science.org at Texas A&M University, Kingsville on November 14, 2025

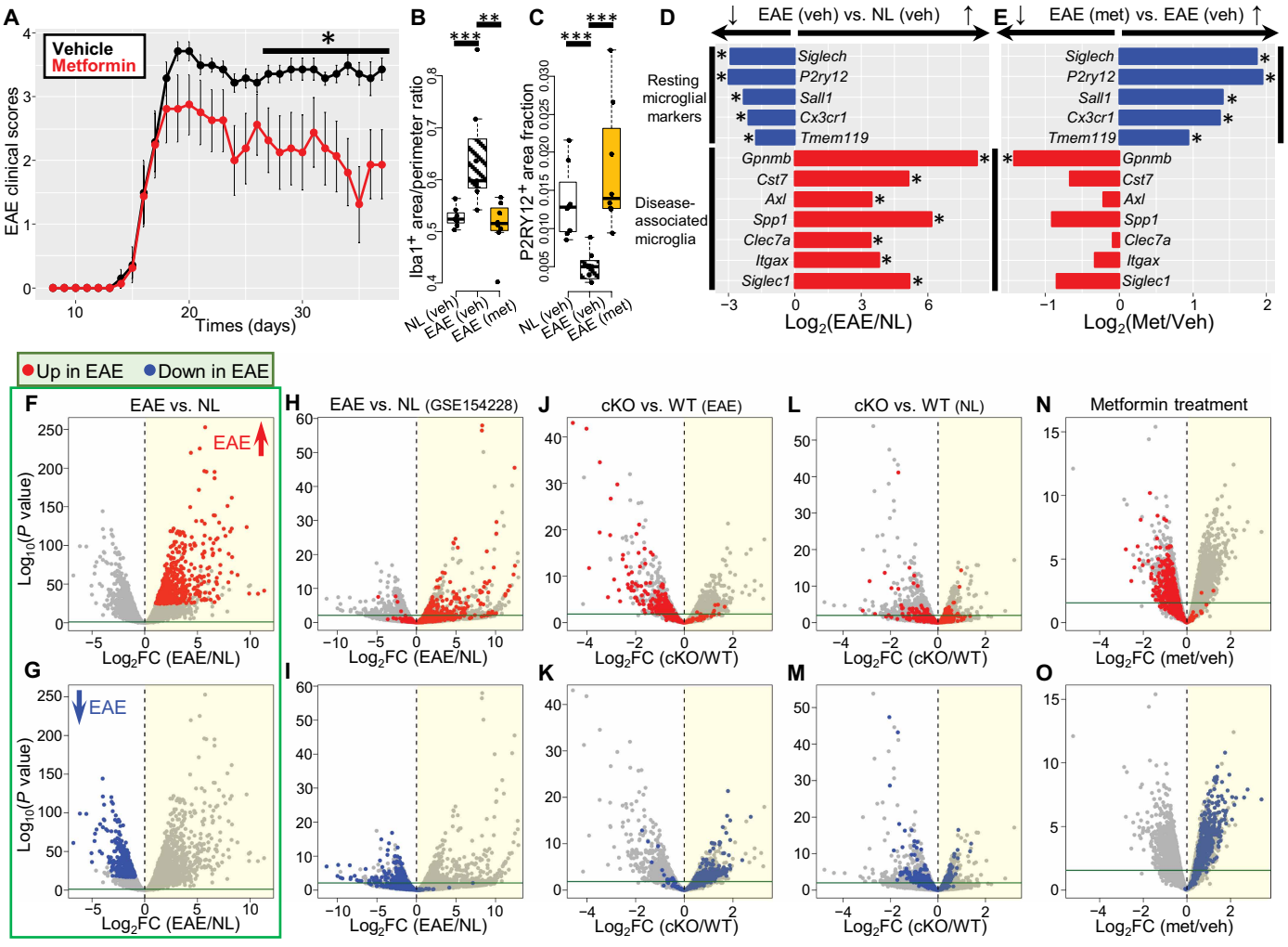

Fig. 5. Metformin treatment is protective during EAE in female mice. (**A**) Shown are EAE clinical scores for metformin- and vehicle-treated female EAE mice. $n = 7$ or 8 per group. Repeated-measures one-way ANOVA, $^{*}P < 0.05$. (**B**) Area/perimeter ratios of Iba1^{+} microglia in WT healthy normal control, EAE, and metformin-treated EAE female mice. (**C**) Area fractions of P2RY12^{+} microglia for the same treatment groups as in (B). $n = 7$ or 8 per group. Mann-Whitney U test, $^{**}P < 0.01$; $^{***}P < 0.001$. (**D** and **E**) Gene expression changes in markers for resting microglia (blue) and markers of DAM (red) in EAE versus healthy control mice (D) and metformin-treated versus vehicle-treated EAE mice (E). Asterisk indicates FDR < 0.1 (edgeR). (**F** and **G**) Volcano plots depicting all differentially expressed genes (gray dots). Top 500 EAE-associated up-regulated (F) and down-regulated (G) genes are highlighted in red and blue, respectively. (**H** and **I**) Cross-validation of EAE-associated genes using the GSE154228 dataset. (**J** to **O**) Volcano plots showing differentially up- and down-regulated genes in *Kdm6a* cKO versus WT EAE mice (J and K), in cKO versus WT healthy normal control mice (L and M), and in metformin-treated versus vehicle-treated WT EAE mice (N and O).

up-regulated (Fig. 5F, red) and blue when down-regulated (Fig. 5G, blue) during EAE. These same up-regulated (red) and down-regulated (blue) genes shown in Fig. 5 (F and G) (green box) were then shown in additional volcano plots to track changes in the same genes during other comparisons. First, EAE-associated genes from the analysis of GSE154228 (shown as volcano plots in Fig. 5, H and I) were found to be similar to the genes identified in the EAE experiment here (Fig. 5, F and G). When *Kdm6a* was deleted in microglia during EAE, EAE-associated up-regulated genes (red) were down-regulated, whereas EAE-associated down-regulated genes (blue) were up-regulated (Fig. 5, J and K). This showed reversal of EAE-induced gene expression when *Kdm6a* was selectively deleted from microglia. These gene expression changes were not observed in healthy mice (Fig. 5, L and M). Analogously, metformin treatment of EAE caused most of the EAE-associated up-regulated genes (red) to be down-regulated and most of the EAE-associated down-regulated genes (blue) to be up-regulated (Fig. 5, N and O). Thus, deletion of *Kdm6a* in microglia during EAE and metformin treatment of EAE each reversed gene expression changes induced by EAE. Gene expression changes induced by microglial *Kdm6a* cKO and by metformin treatment in WT were positively correlated ($R = 0.49$, $P < 2.2 \times 10^{-16}$) (fig. S7).

We next determined whether there was a sex difference in the effect of metformin treatment of chronic EAE. Females showed a protective effect of metformin treatment in two additional experiments (scored from disease onset to euthanasia at day 40 or 43 postinduction), whereas males did not (fig. S8, A to C, and table S5). However, when statistical analyses were focused only on the onset of disease (days 17 to 21 postinduction), both females and males showed a protective effect of metformin treatment (female, $P = 0.017$

Downloaded from https://www.science.org at Texas A&M University, Kingsville on November 14, 2025

and $P = 0.001$; male, $P = 0.018$ and $P = 0.0000006$). This was consistent with a previous report showing no sex difference in the protective effect of metformin treatment early in disease induction (up to day 21) (*58*).

Gene expression changes and KDM6A protein binding

To investigate the relationship between translatomics and epigenetics, KDM6A-binding sites were identified using microglial INTACT (isolation of nuclei tagged in specific cell types) and CUT&RUN sequencing (CUT&RUN-seq). *Tmem119*-Cre/ERT2 and CAG-Sun1/sfGFP mice were crossed to specifically label the microglial nuclei, and the specificity of nuclear tag expression was examined using immunohistochemistry on *Tmem119*-Cre/ERT2-CAG-Sun1/sfGFP mice. GFP protein was exclusively expressed in the nuclei of microglia colabeled by P2RY12 and Iba1 (Fig. 6A). Then, spinal cord microglial nuclei were isolated from *Tmem119*-Cre/ERT2-CAG-Sun1/sfGFP mice, and KDM6A-binding sites were identified by CUT&RUN using anti-KDM6A antibody. In EAE mice, genes with KDM6A binding showed a change in expression upon deletion of *Kdm6a* in microglia (Fig. 6, B and C). In the top down-regulated pathway, the inflammatory response pathway, seven genes showed KDM6A binding in EAE (Fig. 6, D and E). In the top up-regulated pathway, transsynaptic signaling, 25 genes showed KDM6A binding in EAE (fig. S9).

The transcriptome in microglia from patients with MS and healthy controls

Expression of *KDM6A* was then examined using human microglial single-nucleus RNA-seq data from UCSC Cell Browser (*59*, *60*). In human microglia, the expression of *KDM6A* was higher in women compared with men with MS (Fig. 7A), aligning with the ability of *KDM6A* to escape X inactivation. The numbers of differentially expressed genes comparing microglia from patients with MS and healthy controls were higher in women than men (Fig. 7B). GO enrichment analysis revealed that up-regulated microglial genes in women with MS were enriched in immune response categories (Fig. 7C). This observation in MS women was a mirror image of that observed during comparison of selective deletion of *Kdm6a* in microglia versus WT in female EAE mice, where there was down-regulation of immune response genes (Fig. 2I). In the top GO category in humans, the immune effector process pathway, there were seven genes that corresponded with KDM6A binding in mice (Fig. 7D).

DISCUSSION

Here, we investigated whether sex differences in the expression of the X-chromosomal gene *Kdm6a* in microglia could contribute to the increased susceptibility of women to MS. We show that microglia-specific KO of *Kdm6a* ameliorated EAE in female but not male mice. Selective deletion of *Kdm6a* in microglia down-regulated DAM markers, up-regulated resting microglial markers, and reversed other translatomic changes induced by EAE in female mice. In addition, metformin treatment ameliorated EAE in female mice and partially normalized translatomic and morphological changes in microglia. Last, transcriptomic analysis of human microglia showed higher expression of *KDM6A* in microglia derived from women compared with men and revealed that more microglial genes were dysregulated in women than in men.

The GTEx found that 37% of all genes exhibit sex-biased expression, and this was tissue specific and brain region specific (*20*–*22*). A sex bias in gene expression depending on brain region is consistent with sex differences in brain substructure volumes (*61*–*73*), and there are sex differences in the brain at the cellular, molecular, and functional levels (*74*–*77*). This suggests that mechanisms of neurodegeneration

Downloaded from https://www.science.org at Texas A&M University, Kingsville on November 14, 2025

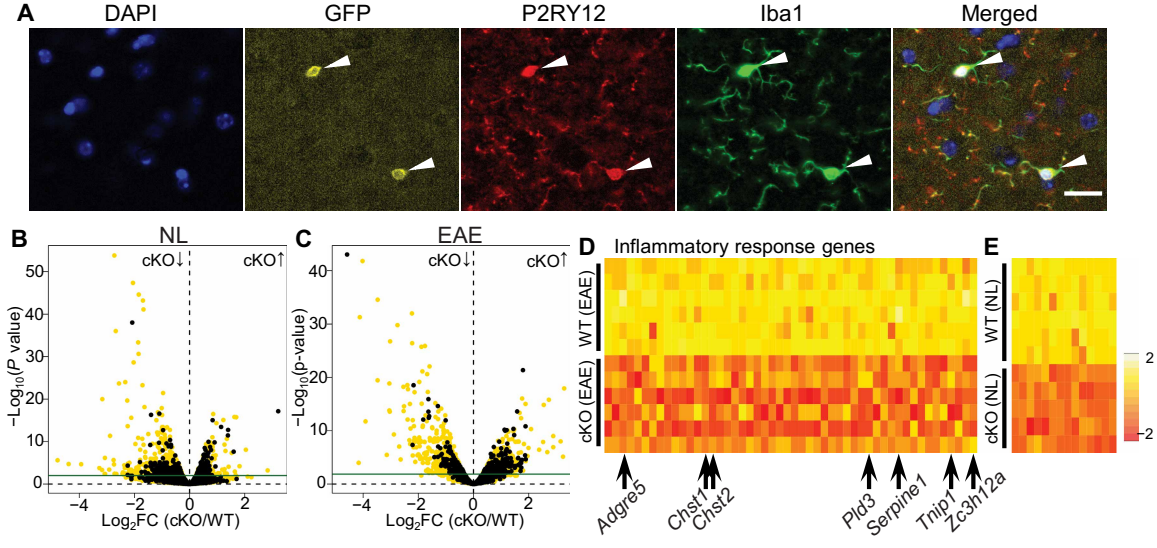

Fig. 6. Correspondence between gene expression changes and KDM6A protein binding. (**A**) Specificity of nuclear tag was examined in *Tmem119*-Cre/ERT2-CAG-Sun1/sfGFP mice. Spinal cord sections were costained with anti-GFP (tagged nuclei; yellow), anti-P2RY12 (red), and anti-Iba1 (green). Arrowheads indicate tagged microglial nuclei. Nuclei, DAPI (blue). Scale bar, 20 μm. (**B** and **C**) CUT&RUN-seq with anti-KDM6A antibody was performed using microglial nuclei immunoprecipitated by the INTACT method. Peaks enriched more than four times higher than immunoglobulin G background were identified as KDM6A-binding loci. The volcano plot depicts differentially translated genes in healthy normal control cKO versus WT female mice (B) or EAE cKO versus WT female mice (C). Black dots show genes with KDM6A binding, and yellow dots show genes without KDM6A binding. (**D** and **E**) Heatmaps of inflammatory response genes (top pathway shown in Fig. 2I): (D) EAE and (E) healthy control. Arrows indicate the genes with KDM6A binding (*Adgre5*, *Chst1*, *Chst2*, *Pld3*, *Serpine1*, *Tnip1*, and *Zc3h12a*). Unit = *z*-score.

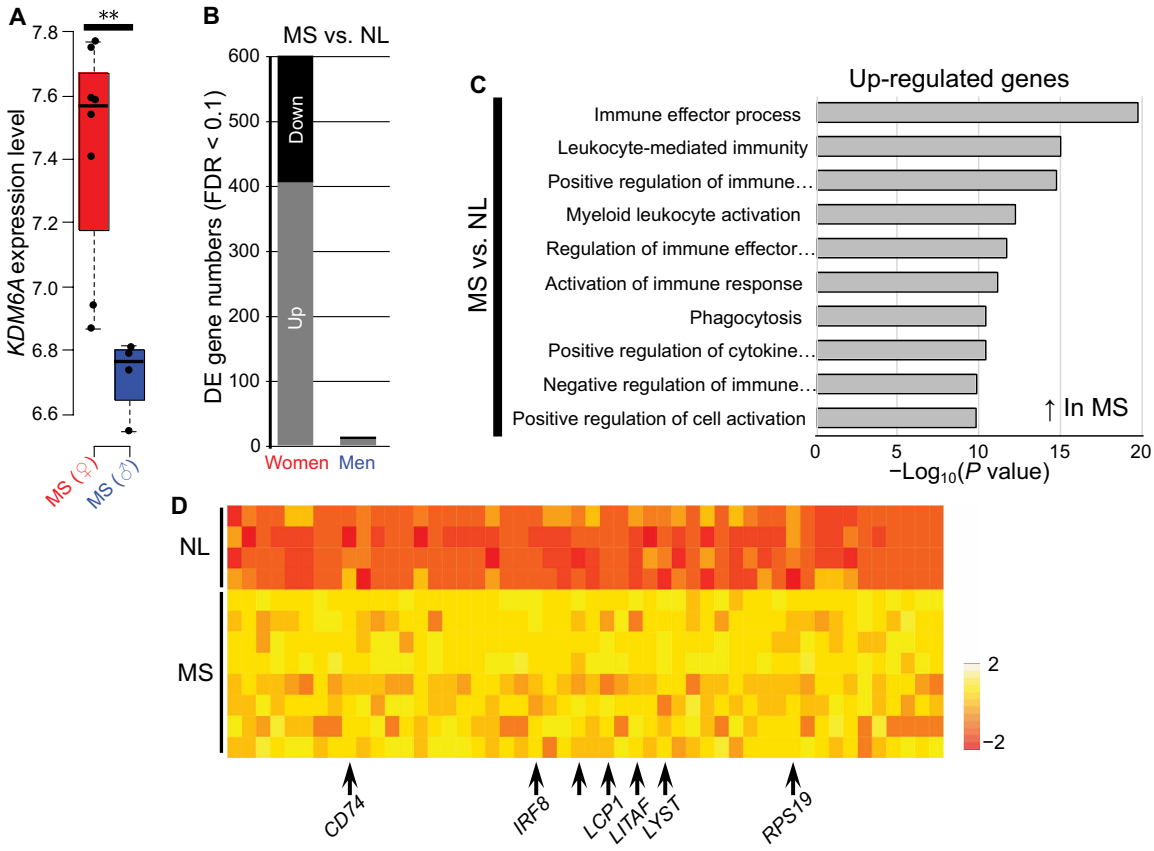

Fig. 7. Sexually dimorphic expression of *KDM6A* in human microglia and disease-related changes in the microglial transcriptome during MS. (**A**) Expression of *KDM6A* in microglia from women compared with microglia from men with MS (one-way ANOVA, $^{**}P < 0.01$). (**B**) Numbers of differentially expressed genes in microglia comparing MS with healthy controls (NL). (**C**) GO enrichment analysis of up-regulated genes (FDR < 0.1 and logFC > 0.5) in microglia of women with MS compared with healthy women. Human brain microglial data from UCSC Cell Browser (https://cells.ucsc.edu/?ds=ms). (**D**) Heatmaps of immune effector process pathway genes. Arrows indicate the genes with KDM6A binding identified by mouse CUT&RUN (*CD74*, *IRF8*, *KMT2E*, *LCP1*, *LITAF*, *LYST*, and *RPS19*). Unit = *z*-score.

are likely to be affected by both sex and brain region. Microglial gene expression is known to differ not only by sex (*7*–*13*) but also by brain region (*78*). Together, these findings prompt the question of whether the effect of the X-chromosomal escapee *Kdm6a* may differ by brain region or cell type. Results here showed a deleterious, proinflammatory role of *Kdm6a* in microglia in spinal cords of mice with EAE. Previously, selective deletion of *Kdm6a* in $CD4^+$ T lymphocytes also ameliorated EAE and showed a proinflammatory role of *Kdm6a* in peripheral immune tissues in females. When *Kdm6a* was selectively deleted from $CD4^+$ T lymphocytes, the transcriptome of $CD4^+$ T lymphocytes showed down-regulation of neuroinflammation signaling pathway genes in females (*27*). A spinal cord injury model also found a deleterious role of *Kdm6a*. Region-specific knockout of *Kdm6a* in the corticospinal tract by injection of adeno-associated virus–Cre–enhanced GFP induced axonal regeneration and functional recovery (*79*–*81*). In contrast, an Alzheimer's disease (AD) model described a protective effect of *Kdm6a* upon lentivirus-mediated expression in the hippocampi of male mice (*82*). A protective effect of *Kdm6a* in the AD model versus a deleterious effect in the MS model may be due to cell-specific, brain region–specific, or disease-specific differences. The sex-specific effects of *Kdm6a* deletion might be explained by a gene-dosage effect, sex-specific differences in the contribution of microglia to EAE, or both. *Kdm6a* might be deleterious in both sexes, but because females have a double dosage of the *Kdm6a* gene compared with males, the impact of cKO or treatment could be higher in females. The effect of selective deletion of *Kdm6a* was more robust in females than males for not only microglia but also for Iba1 and CD3 staining in the spinal cord. In contrast, the effect of *Kdm6a* deletion had no sex difference for measures of axonal damage (APP) and demyelination (MBP). This suggests a deleterious role for *Kdm6a* that is direct for neuroinflammation and indirect for axonal degeneration. This is consistent with a previous report of a disease-promoting effect of *Kdm6a* in $CD4^+$ T cells in EAE females (*27*). Males were not studied in the previous report, but data here suggest that the effect of selection of *Kdm6a* in $CD4^+$ T cells in males would be less robust than the effect in females. This finding is consistent with autoimmune diseases being more prevalent in females compared with males, including systemic lupus erythematosus and rheumatoid arthritis (*83*).

A translationally viable treatment approach for women with MS must consider the mode of delivery. During systemic delivery, an additional beneficial effect of KDM6A inhibition would be expected on the basis of effects on $CD4^+$ T lymphocytes (as discussed above). GSK-J4, a small-molecule inhibitor of KDM6A/6B, has been shown to ameliorate EAE (*84*, *85*). Metformin inhibits the histone demethylase activity of KDM6A (*55*), and treatment with metformin attenuated

Downloaded from https://www.science.org at Texas A&M University, Kingsville on November 14, 2025

EAE and had anti-inflammatory effects in the periphery (*56*, *57*). Here, a protective effect of metformin treatment on microglia during EAE was shown in females but not in males. Clinical trials in MS should be designed in a sex-specific manner because there may be a sex difference in treatment efficacy. An optimal primary outcome measure may be reduction of lesions with paramagnetic phase rims on magnetic resonance imaging because they are thought to represent microglia at the smoldering lesion edge and have been linked to disability progression (*86*).

This study has limitations. Mice do not recapitulate all aspects of the human condition. However, the chronic EAE model shares many neuropathologic features with MS, and it has been used extensively in the development of FDA-approved MS drugs (*38*). In addition, metformin has many functions that are likely independent of inhibiting activity of KDM6A; therefore, a more precise translational strategy to inhibit KDM6A is desirable. We can therefore not conclude that the protective effects of metformin seen in EAE mice are solely attributable to KDM6A inhibition. Last, our analysis of human transcriptomic data showed that microglia from women with MS compared with men with MS had higher *KDM6A* expression, as well as more differentially expressed genes, driven predominantly by immune gene up-regulation in women. Future studies are needed that combine human transcriptomics with epigenetics. One could isolate microglia from women and men with MS and healthy controls, perform gene expression analyses, and identify KDM6A-binding sites. This will reveal whether KDM6A binding drives gene expression changes in microglia of each sex.

In conclusion, clinical observations of a sex difference in neurodegenerative diseases combined with laboratory observations of sex differences in microglia served as the foundation for studying the role of an X-chromosomal gene that escapes X inactivation, namely, *Kdm6a*. Our discovery that selective deletion of *Kdm6a* in microglia reduced clinical EAE and changed the microglial translatome from disease-associated to resting warrants further translational studies investigating this treatment target for women with MS (fig. S10). Although disability progression is worse in men with MS, most patients with MS are women. Thus, treatments are needed that target cells of the brain in both men and women with MS. One should not assume that each sex will respond with equal efficacy to treatment. Trials should be designed and powered to determine the efficacy of treatment in each sex, particularly when the mechanism of action may be influenced by sex chromosome genes or sex hormones. This can lead to optimal neuroprotective strategies tailored for each sex.

MATERIALS AND METHODS

Study design

The objective of this study was to determine the effect of microglial *KDM6A*/*Kdm6a* in EAE mice using knockout of the *Kdm6a* gene in microglia and a RiboTag approach for analysis of the microglial translatome. Age-matched animals were assigned randomly into experimental groups. Sample sizes were based on previous publications with respect to EAE scores and translatome analyses (*27*, *87*). With regard to the sex differences in genotype and treatment, females and males were investigated in the same cohort. Investigators performing the animal experiments were blinded to genotype information. Studies in animals were reviewed and approved by the Chancellor's Animal Research Committee of the University of California, Los Angeles Office for the Protection of Research Subjects (ARC-1998-001). Our study adhered to ARRIVE (Animal Research: Reporting of In Vivo Experiments) guidelines. Single-nucleus RNA-seq data for MS and control CNS cells were obtained from UCSC Cell Browser (https://cells.ucsc.edu/?ds=ms).

Statistical analysis

Statistical analyses and production of figures were performed in R (R Core Team, 2024, www.R-project.org/). Differences in EAE scores between WT and cKO were measured by repeated-measures one-way analysis of variance (ANOVA). Quantitative differences in immunohistochemistry were examined by Mann-Whitney *U* test. *P* values less than 0.05 were considered significant. For gene expression analysis, differentially expressed or translated genes were identified with R package "edgeR" (*88*). An FDR of 0.1 was used as the threshold of differentially expressed or translated genes. GO enrichment analysis was performed using package "clusterProfiler" in R.

Supplementary Materials

The PDF file includes:
Materials and Methods
Figs. S1 to S10
Tables S1, S3 to S5
Legend for table S2
References (*89*–*94*)

Other Supplementary Material for this manuscript includes the following:
Table S2
Data file S1
MDAR Reproducibility Checklist

REFERENCES AND NOTES

1. K. Bjornevik, M. Cortese, B. C. Healy, J. Kuhle, M. J. Mina, Y. Leng, S. J. Elledge, D. W. Niebuhr, A. I. Scher, K. L. Munger, A. Ascherio, Longitudinal analysis reveals high prevalence of Epstein-Barr virus associated with multiple sclerosis. *Science* **375**, 296–301 (2022).
2. L. Moutsianas, L. Jostins, A. H. Beecham, A. T. Dilthey, D. K. Xifara, M. Ban, T. S. Shah, N. A. Patsopoulos, L. Alfredsson, C. A. Anderson, K. E. Attfield, S. E. Baranzini, J. Barrett, T. M. C. Binder, D. Booth, D. Buck, E. G. Celius, C. Cotsapas, S. D'Alfonso, C. A. Dendrou, P. Donnelly, B. Dubois, B. Fontaine, L. Fugger, A. Goris, P.-A. Gourraud, C. Graetz, B. Hemmer, J. Hillert, International IBD Genetics Consortium (IIBDGC), I. Kockum, S. Leslie, C. M. Lill, F. Martinelli-Boneschi, J. R. Oksenberg, T. Olsson, A. Oturai, J. Saarela, H. B. Sondergaard, A. Spurkland, B. Taylor, J. Winkelmann, F. Zipp, J. L. Haines, M. A. Pericak-Vance, C. C. A. Spencer, G. Stewart, D. A. Hafler, A. J. Ivinson, H. F. Harbo, S. L. Hauser, P. L. De Jager, A. Compston, J. L. McCauley, S. Sawcer, G. McVean, Class II HLA interactions modulate genetic risk for multiple sclerosis. *Nat. Genet.* **47**, 1107–1113 (2015).
3. T. Matsushita, L. Madireddy, T. Sprenger, P. Khankhanian, S. Magon, Y. Naegelin, E. Caverzasi, R. L. P. Lindberg, L. Kappos, S. L. Hauser, J. R. Oksenberg, R. Henry, D. Pelletier, S. E. Baranzini, Genetic associations with brain cortical thickness in multiple sclerosis. *Genes Brain Behav.* **14**, 217–227 (2015).
4. R. R. Voskuhl, S. M. Gold, Sex-related factors in multiple sclerosis susceptibility and progression. *Nat. Rev. Neurol.* **8**, 255–263 (2012).
5. S. Hickman, S. Izzy, P. Sen, L. Morsett, J. El Khoury, Microglia in neurodegeneration. *Nat. Neurosci.* **21**, 1359–1369 (2018).
6. F. L. Heppner, M. Greter, D. Marino, J. Falsig, G. Raivich, N. Hovelmeyer, A. Waisman, T. Rulicke, M. Prinz, J. Priller, B. Becher, A. Aguzzi, Experimental autoimmune encephalomyelitis repressed by microglial paralysis. *Nat. Med.* **11**, 146–152 (2005).
7. C. I. Delage, E. Simoncicova, M. E. Tremblay, Microglial heterogeneity in aging and Alzheimer's disease: Is sex relevant? *J. Pharmacol. Sci.* **146**, 169–181 (2021).
8. J. L. Bollinger, Uncovering microglial pathways driving sex-specific neurobiological effects in stress and depression. *Brain Behav. Immun. Health* **16**, 100320 (2021).
9. N. Yanguas-Casás, A. Crespo-Castrillo, M.-A. Arevalo, L. M. Garcia-Segura, Aging and sex: Impact on microglia phagocytosis. *Aging Cell* **19**, e13182 (2020).
10. C. W. Hui, H. A. Vecchiarelli, E. Gervais, X. Luo, F. Michaud, L. Scheefhals, K. Bisht, K. Sharma, L. Topolnik, M. E. Tremblay, Sex differences of microglia and synapses in the hippocampal dentate gyrus of adult mouse offspring exposed to maternal immune activation. *Front. Cell. Neurosci.* **14**, 558181 (2020).

Downloaded from https://www.science.org at Texas A&M University, Kingsville on November 14, 2025

11. C. Sala Frigerio, L. Wolfs, N. Fattorelli, N. Thrupp, I. Voytyuk, I. Schmidt, R. Mancuso, W.-T. Chen, M. E. Woodbury, G. Srivastava, T. Möller, E. Hudry, S. Das, T. Saido, E. Karran, B. Hyman, V. H. Perry, M. Fiers, B. De Strooper, The major risk factors for Alzheimer's disease: Age, sex, and genes modulate the microglia response to Aβ plaques. *Cell Rep.* **27**, 1293–1306.e6 (2019).
12. A. Villa, P. Gelosa, L. Castiglioni, M. Cimino, N. Rizzi, G. Pepe, F. Lolli, E. Marcello, L. Sironi, E. Vegeto, A. Maggi, Sex-specific features of microglia from adult mice. *Cell Rep.* **23**, 3501–3511 (2018).
13. C. A. Mangold, B. Wronowski, M. Du, D. R. Masser, N. Hadad, G. V. Bixler, R. M. Brucklacher, M. M. Ford, W. E. Sonntag, W. M. Freeman, Sexually divergent induction of microglial-associated neuroinflammation with hippocampal aging. *J. Neuroinflammation* **14**, 141 (2017).
14. D. L. Smith-Bouvier, A. A. Divekar, M. Sasidhar, S. Du, S. K. Tiwari-Woodruff, J. K. King, A. P. Arnold, R. R. Singh, R. R. Voskuhl, A role for sex chromosome complement in the female bias in autoimmune disease. *J. Exp. Med.* **205**, 1099–1108 (2008).
15. M. V. Sasidhar, N. Itoh, S. M. Gold, G. W. Lawson, R. R. Voskuhl, The XX sex chromosome complement in mice is associated with increased spontaneous lupus compared with XY. *Ann. Rheum. Dis.* **71**, 1418–1422 (2012).
16. C. Teuscher, R. Noubade, K. Spach, B. McElvany, J. Y. Bunn, P. D. Fillmore, J. F. Zachary, E. P. Blankenhorn, Evidence that the Y chromosome influences autoimmune disease in male and female mice. *Proc. Natl. Acad. Sci. U.S.A.* **103**, 8024–8029 (2006).
17. R. Voskuhl, S. Klein, Sex is a biological variable - in the brain too. *Nature* **568**, 171 (2019).
18. A. Youness, C.-H. Miquel, J.-C. Guéry, Escape from X chromosome inactivation and the female predominance in autoimmune diseases. *Int. J. Mol. Sci.* **22**, 1114 (2021).
19. R. Voskuhl, Y. Itoh, The X factor in neurodegeneration. *J. Exp. Med.* **219**, e20211488 (2022).
20. S. Kim-Hellmuth, F. Aguet, M. Oliva, M. Muñoz-Aguirre, S. Kasela, V. Wucher, S. E. Castel, A. R. Hamel, A. Viñuela, A. L. Roberts, S. Mangul, X. Wen, G. Wang, A. N. Barbeira, D. Garrido-Martín, B. B. Nadel, Y. Zou, R. Bonazzola, J. Quan, A. Brown, A. Martinez-Perez, J. M. Soria, GTex Consortium, G. Getz, E. T. Dermitzakis, K. S. Small, M. Stephens, H. S. Xi, H. K. Im, R. Guigó, A. V. Segrè, B. E. Stranger, K. G. Ardlie, T. Lappalainen, Cell type–specific genetic regulation of gene expression across human tissues. *Science* **369**, eaaz8528 (2020).
21. M. Oliva, M. Muñoz-Aguirre, S. Kim-Hellmuth, V. Wucher, A. D. H. Gewirtz, D. J. Cotter, P. Parsana, S. Kasela, B. Balliu, A. Viñuela, S. E. Castel, P. Mohammadi, F. Aguet, Y. Zou, E. A. Khramtsova, A. D. Skol, D. Garrido-Martín, F. Reverter, A. Brown, P. Evans, E. R. Gamazon, A. Payne, R. Bonazzola, A. N. Barbeira, A. R. Hamel, A. Martinez-Perez, J. M. Soria, GTex Consortium, B. L. Pierce, M. Stephens, E. Eskin, E. T. Dermitzakis, A. V. Segrè, H. K. Im, B. E. Engelhardt, K. G. Ardlie, S. B. Montgomery, A. J. Battle, T. Lappalainen, R. Guigó, B. E. Stranger, The impact of sex on gene expression across human tissues. *Science* **369**, eaba3066 (2020).
22. C. M. Lopes-Ramos, C. Y. Chen, M. L. Kuijjer, J. N. Paulson, A. R. Sonawane, M. Fagny, J. Platig, K. Glass, J. Quackenbush, D. L. DeMeo, Sex differences in gene expression and regulatory networks across 29 human tissues. *Cell Rep.* **31**, 107795 (2020).
23. R. R. Voskuhl, N. Itoh, A. Tassoni, M. A. Matsukawa, E. Ren, V. Tse, E. Jang, T. T. Suen, Y. Itoh, Gene expression in oligodendrocytes during remyelination reveals cholesterol homeostasis as a therapeutic target in multiple sclerosis. *Proc. Natl. Acad. Sci. U.S.A.* **116**, 10130–10139 (2019).
24. J. P. An, R. C. J. Ribeiro, P. Webb, J. A. Gustafsson, P. J. Kushner, J. D. Baxter, D. C. Leitman, Estradiol repression of tumor necrosis factor-α transcription requires estrogen receptor activation function-2 and is enhanced by coactivators. *Proc. Natl. Acad. Sci. U.S.A.* **96**, 15161–15166 (1999).
25. Y. Meng, L. Zong, Estrogen stimulates SREBP2 expression in hepatic cell lines via an estrogen response element in the SREBP2 promoter. *Cell. Mol. Biol. Lett.* **24**, 65 (2019).
26. P. M. I. A. Doss, M. Umair, J. Baillargeon, R. Fazazi, N. Fudge, I. Akbar, A. P. Yeola, J. B. Williams, M. Leclercq, C. Joly-Beauparlant, P. Beauchemin, G. F. Ruda, M. Alpaugh, A. C. Anderson, P. E. Brennan, A. Droit, H. Lassmann, C. S. Moore, M. Rangachari, Male sex chromosomal complement exacerbates the pathogenicity of Th17 cells in a chronic model of central nervous system autoimmunity. *Cell Rep.* **34**, 108833 (2021).
27. Y. Itoh, L. C. Golden, N. Itoh, M. A. Matsukawa, E. Ren, V. Tse, A. P. Arnold, R. R. Voskuhl, The X-linked histone demethylase *Kdm6a* in $CD4^+$ T lymphocytes modulates autoimmunity. *J. Clin. Invest.* **129**, 3852–3863 (2019).
28. S. Horvath, DNA methylation age of human tissues and cell types. *Genome Biol.* **14**, R115 (2013).
29. K. M. Palaszynski, D. L. Smith, S. Kamrava, P. S. Burgoyne, A. P. Arnold, R. R. Voskuhl, A Yin-Yang effect between sex chromosome complement and sex hormones on the immune response. *Endocrinology* **146**, 3280–3285 (2005).
30. G. J. De Vries, Sex steroids and sex chromosomes at odds? *Endocrinology* **146**, 3277–3279 (2005).
31. G. D. Penny, G. F. Kay, S. A. Sheardown, S. Rastan, N. Brockdorff, Requirement for Xist in X chromosome inactivation. *Nature* **379**, 131–137 (1996).
32. A. Greenfield, L. Carrel, D. Pennisi, C. Philippe, N. Quaderi, P. Siggers, K. Steiner, P. P. L. Tam, A. P. Monaco, H. F. Willard, P. Koopman, The UTX gene escapes X inactivation in mice and humans. *Hum. Mol. Genet.* **7**, 737–742 (1998).
33. J. Xu, X. X. Deng, R. Watkins, C. M. Disteche, Sex-specific differences in expression of histone demethylases Utx and Uty in mouse brain and neurons. *J. Neurosci.* **28**, 4521–4527 (2008).
34. I. Issaeva, Y. Zonis, T. Rozovskaia, K. Orlovsky, C. M. Croce, T. Nakamura, A. Mazo, L. Eisenbach, E. Canaani, Knockdown of ALR (MLL2) reveals ALR target genes and leads to alterations in cell adhesion and growth. *Mol. Cell. Biol.* **27**, 1889–1903 (2007).
35. S. S. Dhar, S. H. Lee, P. Y. Kan, P. Voigt, L. Ma, X. Shi, D. Reinberg, M. G. Lee, Trans-tail regulation of MLL4-catalyzed H3K4 methylation by H4R3 symmetric dimethylation is mediated by a tandem PHD of MLL4. *Genes Dev.* **26**, 2749–2762 (2012).
36. S. Hong, Y. W. Cho, L. R. Yu, H. Yu, T. D. Veenstra, K. Ge, Identification of JmjC domain-containing UTX and JMJD3 as histone H3 lysine 27 demethylases. *Proc. Natl. Acad. Sci. U.S.A.* **104**, 18439–18444 (2007).
37. S. Seenundun, S. Rampalli, Q. C. Liu, A. Aziz, C. Palii, S. Hong, A. Blais, M. Brand, K. Ge, F. J. Dilworth, UTX mediates demethylation of H3K27me3 at muscle-specific genes during myogenesis. *EMBO J.* **29**, 1401–1411 (2010).
38. R. R. Voskuhl, A. MacKenzie-Graham, Chronic experimental autoimmune encephalomyelitis is an excellent model to study neuroaxonal degeneration in multiple sclerosis. *Front. Mol. Neurosci.* **15**, 1024058 (2022).
39. C. S. Constantinescu, N. Farooqi, K. O'Brien, B. Gran, Experimental autoimmune encephalomyelitis (EAE) as a model for multiple sclerosis (MS). *Br. J. Pharmacol.* **164**, 1079–1106 (2011).
40. S. Yona, K. W. Kim, Y. Wolf, A. Mildner, D. Varol, M. Breker, D. Strauss-Ayali, S. Viukov, M. Guilliams, A. Misharin, D. A. Hume, H. Perlman, B. Malissen, E. Zelzer, S. Jung, Fate mapping reveals origins and dynamics of monocytes and tissue macrophages under homeostasis. *Immunity* **38**, 79–91 (2013).
41. M. L. Bennett, F. C. Bennett, S. A. Liddelow, B. Ajami, J. L. Zamanian, N. B. Fernhoff, S. B. Mulinyawe, C. J. Bohlen, A. Adil, A. Tucker, I. L. Weissman, E. F. Chang, G. Li, G. A. Grant, M. G. Hayden Gephart, B. A. Barres, New tools for studying microglia in the mouse and human CNS. *Proc. Natl. Acad. Sci. U.S.A.* **113**, E1738–E1746 (2016).
42. T. Kaiser, G. Feng, Tmem119-EGFP and Tmem119-CreERT2 transgenic mice for labeling and manipulating microglia. *eNeuro* **6**, ENEURO.0448-18.2019 (2019).
43. T. Goldmann, P. Wieghofer, P. F. Müller, Y. Wolf, D. Varol, S. Yona, S. M. Brendecke, K. Kierdorf, O. Staszewski, M. Datta, T. Luedde, M. Heikenwalder, S. Jung, M. Prinz, A new type of microglia gene targeting shows TAK1 to be pivotal in CNS autoimmune inflammation. *Nat. Neurosci.* **16**, 1618–1626 (2013).
44. A. E. Cardona, E. P. Pioro, M. E. Sasse, V. Kostenko, S. M. Cardona, I. M. Dijkstra, D. Huang, G. Kidd, S. Dombrowski, R. Dutta, J. C. Lee, D. N. Cook, S. Jung, S. A. Lira, D. R. Littman, R. M. Ransohoff, Control of microglial neurotoxicity by the fractalkine receptor. *Nat. Neurosci.* **9**, 917–924 (2006).
45. L. Hertwig, I. Hamann, S. Romero-Suarez, J. M. Millward, R. Pietrek, C. Chanvillard, H. Stuis, K. Pollok, R. M. Ransohoff, A. E. Cardona, C. Infante-Duarte, CX3CR1-dependent recruitment of mature NK cells into the central nervous system contributes to control autoimmune neuroinflammation. *Eur. J. Immunol.* **46**, 1984–1996 (2016).
46. D. Huang, F. D. Shi, S. Jung, G. C. Pien, J. Wang, T. P. Salazar-Mather, T. T. He, J. T. Weaver, H. G. Ljunggren, C. A. Biron, D. R. Littman, R. M. Ransohoff, The neuronal chemokine CX3CL1/fractalkine selectively recruits NK cells that modify experimental autoimmune encephalomyelitis within the central nervous system. *FASEB J.* **20**, 896–905 (2006).
47. W. Mai, X. Liu, J. Wang, J. Zheng, X. Wang, W. Zhou, Protective effects of CX3CR1 on autoimmune inflammation in a chronic EAE model for MS through modulation of antigen-presenting cell-related molecular MHC-II and its regulators. *Neurol. Sci.* **40**, 779–791 (2019).
48. E. Sanz, J. C. Bean, D. P. Carey, A. Quintana, G. S. McKnight, RiboTag: Ribosomal tagging strategy to analyze cell-type-specific mRNA expression in vivo. *Curr. Protoc. Neurosci.* **88**, e77 (2019).
49. T. E. Faust, P. A. Feinberg, C. O'Connor, R. Kawaguchi, A. Chan, H. Strasburger, M. Frosch, M. A. Boyle, T. Masuda, L. Amann, K.-P. Knobeloch, M. Prinz, A. Schaefer, D. P. Schafer, A comparative analysis of microglial inducible Cre lines. *Cell Rep.* **42**, 113031 (2023).
50. M. Zelic, F. Pontarelli, L. Woodworth, C. Zhu, A. Mahan, Y. Ren, M. LaMorte, R. Gruber, A. Keane, P. Loring, L. Guo, T. H. Xia, B. Zhang, P. Orning, E. Lien, A. Degterev, T. Hammond, D. Ofengeim, RIPK1 activation mediates neuroinflammation and disease progression in multiple sclerosis. *Cell Rep.* **35**, 109112 (2021).
51. W. M. Song, M. Colonna, The identity and function of microglia in neurodegeneration. *Nat. Immunol.* **19**, 1048–1058 (2018).
52. J. F. J. Bogie, E. Boelen, E. Louagie, P. Delputte, D. Elewaut, J. van Horssen, J. J. A. Hendriks, N. Hellings, CD169 is a marker for highly pathogenic phagocytes in multiple sclerosis. *Mult. Scler. J.* **24**, 290–300 (2018).
53. S. George, N. L. Rey, T. Tyson, C. Esquibel, L. Meyerdirk, E. Schulz, S. Pierce, A. R. Burmeister, Z. Madaj, J. A. Steiner, M. L. Escobar Galvis, L. Brundin, P. Brundin, Microglia affect α-synuclein cell-to-cell transfer in a mouse model of Parkinson's disease. *Mol. Neurodegener.* **14**, 34 (2019).
54. C. Ma, S. Li, Y. Hu, Y. Ma, Y. Wu, C. Wu, X. Liu, B. Wang, G. Hu, J. Zhou, S. Yang, AIM2 controls microglial inflammation to prevent experimental autoimmune encephalomyelitis. *J. Exp. Med.* **218**, e20201796 (2021).

Downloaded from https://www.science.org at Texas A&M University, Kingsville on November 14, 2025

55. E. Cuyàs, S. Verdura, L. Llorach-Pares, S. Fernández-Arroyo, F. Luciano-Mateo, N. Cabré, J. Stursa, L. Werner, B. Martin-Castillo, B. Viollet, J. Neuzil, J. Joven, A. Nonell-Canals, M. Sanchez-Martinez, J. A. Menendez, Metformin directly targets the H3K27me3 demethylase KDM6A/UTX. *Aging Cell* **17**, e12772 (2018).
56. N. Nath, M. Khan, M. K. Paintlia, I. Singh, M. N. Hoda, S. Giri, Metformin attenuated the autoimmune disease of the central nervous system in animal models of multiple sclerosis. *J. Immunol.* **182**, 8005–8014 (2009).
57. Y. F. Sun, T. Tian, J. Gao, X. Q. Liu, H. Q. Hou, R. J. Cao, B. Li, M. Y. Quan, L. Guo, Metformin ameliorates the development of experimental autoimmune encephalomyelitis by regulating T helper 17 and regulatory T cells in mice. *J. Neuroimmunol.* **292**, 58–67 (2016).
58. E. A. B. Gilbert, J. Livingston, E. G. Flores, M. Khan, H. Kandavel, C. M. Morshead, Metformin treatment reduces inflammation, dysmyelination and disease severity in a mouse model of multiple sclerosis, experimental autoimmune encephalomyelitis. *Brain Res.* **1822**, 148648 (2024).
59. L. Schirmer, D. Velmeshev, S. Holmqvist, M. Kaufmann, S. Werneburg, D. Jung, S. Vistnes, J. H. Stockley, A. Young, M. Steindel, B. Tung, N. Goyal, A. Bhaduri, S. Mayer, J. B. Engler, O. A. Bayraktar, R. J. M. Franklin, M. Haeussler, R. Reynolds, D. P. Schafer, M. A. Friese, L. R. Shiow, A. R. Kriegstein, D. H. Rowitch, Neuronal vulnerability and multilineage diversity in multiple sclerosis. *Nature* **573**, 75–82 (2019).
60. M. L. Speir, A. Bhaduri, N. S. Markov, P. Moreno, T. J. Nowakowski, I. Papatheodorou, A. A. Pollen, B. J. Raney, L. Seninge, W. J. Kent, M. Haeussler, UCSC Cell Browser: Visualize your single-cell data. *Bioinformatics* **37**, 4578–4580 (2021).
61. C. Corre, M. Friedel, D. A. Vousden, A. Metcalf, S. Spring, L. R. Qiu, J. P. Lerch, M. R. Palmert, Separate effects of sex hormones and sex chromosomes on brain structure and function revealed by high-resolution magnetic resonance imaging and spatial navigation assessment of the Four Core Genotype mouse model. *Brain Struct. Funct.* **221**, 997–1016 (2016).
62. F. Kurth, L. Jancke, E. Luders, Sexual dimorphism of Broca's region: More gray matter in female brains in Brodmann areas 44 and 45. *J. Neurosci. Res.* **95**, 626–632 (2017).
63. F. Kurth, D. Spencer, M. Hines, E. Luders, Sex differences in associations between spatial ability and corpus callosum morphology. *J. Neurosci. Res.* **96**, 1380–1387 (2018).
64. F. Kurth, P. M. Thompson, E. Luders, Investigating the differential contributions of sex and brain size to gray matter asymmetry. *Cortex* **99**, 235–242 (2018).
65. E. Luders, C. Gaser, K. L. Narr, A. W. Toga, Why sex matters: Brain size independent differences in gray matter distributions between men and women. *J. Neurosci.* **29**, 14265–14270 (2009).
66. E. Luders, K. L. Narr, P. M. Thompson, D. E. Rex, L. Jancke, H. Steinmetz, A. W. Toga, Gender differences in cortical complexity. *Nat. Neurosci.* **7**, 799–800 (2004).
67. E. Luders, K. L. Narr, P. M. Thompson, R. P. Woods, D. E. Rex, L. Jancke, H. Steinmetz, A. W. Toga, Mapping cortical gray matter in the young adult brain: Effects of gender. *Neuroimage* **26**, 493–501 (2005).
68. E. Luders, H. Steinmetz, L. Jancke, Brain size and grey matter volume in the healthy human brain. *Neuroreport* **13**, 2371–2374 (2002).
69. E. Luders, A. W. Toga, Sex differences in brain anatomy. *Prog. Brain Res.* **186**, 3–12 (2010).
70. E. Luders, A. W. Toga, P. M. Thompson, Why size matters: Differences in brain volume account for apparent sex differences in callosal anatomy: The sexual dimorphism of the corpus callosum. *Neuroimage* **84**, 820–824 (2014).
71. C. E. Meyer, F. Kurth, S. Lepore, J. L. Gao, H. Johnsonbaugh, M. R. Oberoi, S. J. Sawiak, A. MacKenzie-Graham, In vivo magnetic resonance images reveal neuroanatomical sex differences through the application of voxel-based morphometry in C57BL/6 mice. *Neuroimage* **163**, 197–205 (2017).
72. O. R. Phillips, K. A. Clark, E. Luders, R. Azhir, S. H. Joshi, R. P. Woods, J. C. Mazziotta, A. W. Toga, K. L. Narr, Superficial white matter: Effects of age, sex, and hemisphere. *Brain Connect.* **3**, 146–159 (2013).
73. S. Spring, J. P. Lerch, R. M. Henkelman, Sexual dimorphism revealed in the structure of the mouse brain using three-dimensional magnetic resonance imaging. *Neuroimage* **35**, 1424–1433 (2007).
74. M. M. McCarthy, C. S. Woolley, A. P. Arnold, Incorporating sex as a biological variable in neuroscience: What do we gain? *Nat. Rev. Neurosci.* **18**, 707–708 (2017).
75. S. Weis, K. R. Patil, F. Hoffstaedter, A. Nostro, B. T. T. Yeo, S. B. Eickhoff, Sex classification by resting state brain connectivity. *Cereb. Cortex* **30**, 824–835 (2020).
76. D. Scheinost, E. S. Finn, F. Tokoglu, X. Shen, X. Papademetris, M. Hampson, R. T. Constable, Sex differences in normal age trajectories of functional brain networks. *Hum. Brain Mapp.* **36**, 1524–1535 (2015).
77. T. D. Satterthwaite, D. H. Wolf, D. R. Roalf, K. Ruparel, G. Erus, S. Vandekar, E. D. Gennatas, M. A. Elliott, A. Smith, H. Hakonarson, Linked sex differences in cognition and functional connectivity in youth. *Cereb. Cortex* **25**, 2383–2394 (2015).
78. K. Grabert, T. Michoel, M. H. Karavolos, S. Clohisey, J. K. Baillie, M. P. Stevens, T. C. Freeman, K. M. Summers, B. W. McColl, Microglial brain region-dependent diversity and selective regional sensitivities to aging. *Nat. Neurosci.* **19**, 504–516 (2016).
79. S. Ni, Z. Luo, L. Jiang, Z. Guo, P. Li, X. Xu, Y. Cao, C. Duan, T. Wu, C. Li, H. Lu, J. Hu, UTX/KDM6A deletion promotes recovery of spinal cord injury by epigenetically regulating vascular regeneration. *Mol. Ther.* **27**, 2134–2146 (2019).
80. Z. Guo, C. Li, Y. Cao, T. Qin, L. Jiang, Y. Xu, M. Li, Z. Luo, J. Hu, H. Lu, UTX/KDM6A deletion promotes the recovery of spinal cord injury by epigenetically triggering intrinsic neural regeneration. *Mol. Ther. Methods Clin. Dev.* **20**, 337–349 (2021).
81. C. Gao, F. Yin, R. Li, Q. Ruan, C. Meng, K. Zhao, Q. Zhu, MicroRNA-145-mediated KDM6A downregulation enhances neural repair after spinal cord injury via the NOTCH2/Abcb1a axis. *Oxid. Med. Cell. Longev.* **2021**, 2580619 (2021).
82. E. J. Davis, L. Broestl, S. Abdulai-Saiku, K. Worden, L. W. Bonham, E. Minones-Moyano, A. J. Moreno, D. Wang, K. Chang, G. Williams, B. I. Garay, I. Lobach, N. Devidze, D. Kim, C. Anderson-Bergman, G. Q. Yu, C. C. White, J. A. Harris, B. L. Miller, D. A. Bennett, A. P. Arnold, P. L. De Jager, J. J. Palop, B. Panning, J. S. Yokoyama, L. Mucke, D. B. Dubal, A second X chromosome contributes to resilience in a mouse model of Alzheimer's disease. *Sci. Transl. Med.* **12**, eaaz5677 (2020).
83. C. C. Whitacre, S. C. Reingold, P. A. O'Looney, A gender gap in autoimmunity. *Science* **283**, 1277–1278 (1999).
84. C. Donas, M. Carrasco, M. Fritz, C. Prado, G. Tejon, F. Osorio-Barrios, V. Manriquez, P. Reyes, R. Pacheco, M. R. Bono, A. Loyola, M. Rosemblatt, The histone demethylase inhibitor GSK-J4 limits inflammation through the induction of a tolerogenic phenotype on DCs. *J. Autoimmun.* **75**, 105–117 (2016).
85. J. Abu-Hanna, J. A. Patel, E. Anastasakis, R. Cohen, L. H. Clapp, M. Loizidou, M. M. R. Eddama, Therapeutic potential of inhibiting histone 3 lysine 27 demethylases: A review of the literature. *Clin. Epigenetics* **14**, 98 (2022).
86. M. Absinta, D. Maric, M. Gharagozloo, T. Garton, M. D. Smith, J. Jin, K. C. Fitzgerald, A. Song, P. Liu, J. P. Lin, T. Wu, K. R. Johnson, D. B. McGavern, D. P. Schafer, P. A. Calabresi, D. S. Reich, A lymphocyte-microglia-astrocyte axis in chronic active multiple sclerosis. *Nature* **597**, 709–714 (2021).
87. N. Itoh, Y. Itoh, A. Tassoni, E. Ren, M. Kaito, A. Ohno, Y. Ao, V. Farkhondeh, H. Johnsonbaugh, J. Burda, M. V. Sofroniew, R. R. Voskuhl, Cell-specific and region-specific transcriptomics in the multiple sclerosis model: Focus on astrocytes. *Proc. Natl. Acad. Sci. U.S.A.* **115**, E302–E309 (2018).
88. M. D. Robinson, D. J. McCarthy, G. K. Smyth, edgeR: A Bioconductor package for differential expression analysis of digital gene expression data. *Bioinformatics* **26**, 139–140 (2010).
89. R. D. Spence, M. E. Hamby, E. Umeda, N. Itoh, S. M. Du, A. J. Wisdom, Y. Cao, G. Bondar, J. Lam, Y. Ao, F. Sandoval, S. Suriany, M. V. Sofroniew, R. R. Voskuhl, Neuroprotection mediated through estrogen receptor-alpha in astrocytes. *Proc. Natl. Acad. Sci. U.S.A.* **108**, 8867–8872 (2011).
90. H. B. Liu, K. K. Loo, K. Palaszynski, J. Ashouri, D. B. Lubahn, R. R. Voskuhl, Estrogen receptor alpha mediates estrogen's immune protection in autoimmune disease. *J. Immunol.* **171**, 6936–6940 (2003).
91. A. M. Bolger, M. Lohse, B. Usadel, Trimmomatic: A flexible trimmer for Illumina sequence data. *Bioinformatics* **30**, 2114–2120 (2014).
92. D. Gaidatzis, A. Lerch, F. Hahne, M. B. Stadler, QuasR: Quantification and annotation of short reads in R. *Bioinformatics* **31**, 1130–1132 (2015).
93. T. Wu, E. Hu, S. Xu, M. Chen, P. Guo, Z. Dai, T. Feng, L. Zhou, W. Tang, L. Zhan, X. Fu, S. Liu, X. Bo, G. Yu, clusterProfiler 4.0: A universal enrichment tool for interpreting omics data. *Innovation (Camb)* **2**, 100141 (2021).
94. A. T. L. Lun, G. K. Smyth, csaw: A Bioconductor package for differential binding analysis of ChIP-seq data using sliding windows. *Nucleic Acids Res.* **44**, e45 (2016).

Acknowledgments: We thank the Wellcome Trust Sanger Institute Mouse Genetics Project (Sanger MGP) and its funders for providing the mutant mouse line [allele: *Kdm6a*$^{tm2a(EUCOMM)Wtsi}$].
Funding: This work was supported by National Institutes of Health [National Institute of Neurological Disorders and Stroke (NINDS)] R35NS132150 (to R.R.V.), National Institutes of Health (NINDS) RO1NS096748 (to R.R.V.), National Institutes of Health (NINDS) RO1NS109670 (to R.R.V.), Conrad N. Hilton Foundation Grants #18394 (to R.R.V.), Dunk MS Foundation (to R.R.V.), and Nancy Davis–Race to Erase MS Foundation (to Y.I. and R.R.V.). **Author contributions:** Y.I., N.I., S.W., N.H., and R.R.V. contributed to the analysis, interpretation of data, and writing of the manuscript. Y.I. performed EAE inductions and sequencing analyses. Y.I., N.I., S.W., and N.H. performed immunofluorescence staining and statistical analysis. N.I. performed cytokine assay. Y.I. and R.R.V. contributed to the conception and design of the work and the writing and approval of the final manuscript. **Competing interests:** The authors declare that they have no competing interests. **Data and materials availability:** All data associated with this study are in the paper or the Supplementary Materials. Datasets generated during this study are available in the GEO (www.ncbi.nlm.nih.gov/geo/) under the accession number GSE220566 (microglia from the spinal cord, EAE female), GSE246008 (microglia from the spinal cord, EAE female and male), GSE261726 (microglia from the spinal cord, metformin treatment), GSE221400 (enrichment), GSE297367 (microglia from the spinal cord, healthy female), and GSE297450 (microglia from the spinal cord, CUT&RUN-seq).

Submitted 8 May 2024
Resubmitted 5 June 2025
Accepted 22 September 2025
Published 15 October 2025
10.1126/scitranslmed.adq3401

Downloaded from https://www.science.org at Texas A&M University, Kingsville on November 14, 2025